Curing Behavior and Residual Stresses in Polymeric Resins Used for Encapsulanting Electronic Packages

Man-Lung Sham and Jang-Kyo Kim

Department of Mechanical Engineering, Hong Kong University of Science and Technology, Clear Water Bay, Kowloon, Hong Kong

Received 23 April 2004; accepted 9 September 2004
DOI 10.1002/app.21384
Published online 27 January 2005 in Wiley InterScience (www.interscience.wiley.com).

ABSTRACT: Polymeric encapsulants are applied in electronic packages to improve the mechanical/thermal performance and the reliability of packaged devices. During the curing process of encapsulating resin, large residual stresses are generated due to the shrinkage of polymer and the mismatches in the coefficient of thermal expansion (CTE) between various package components. In addition, the rheological properties and curing kinetics of the resin also affect the nature and distribution of residual stresses. In this work, the rheological and curing behavior of encapsulating resins are characterized using an oscillatory rheometer. The resin viscosity is closely monitored against curing temperature excursion, which is correlated to exothermic reaction and weight loss as measured from the DSC and TGA analyses. The evolution of residual stresses in encapsulating resin is evaluated in a bimaterial strip bending experiment (BMSB) *in situ* within a DMA chamber. The CTE values are then calculated based on the thermomechanical analysis, which are well compared with those determined from other sources. A transition temperature, apart from the glass transition temperature, is identified from the study of the changes in resin flexural modulus and residual stress profiles. © 2005 Wiley Periodicals, Inc. J Appl Polym Sci 96: 175–182, 2005

Key words: curing of polymers; rheology; thermal properties; residual stresses; flip chip package

INTRODUCTION

Polymeric encapsulant plays a critical role in integrated circuit (IC) packaging. The encapsulant provides chemical and mechanical protection to the IC chips, allowing higher reliability and longer lifetime of the packaged device under the adverse service environment. In recent years, the flip chip technology has been developed to provide a solution to increasing demands for miniaturization and weight reductions for applications in many portable electronics. As schematically illustrated in Figure 1, the technology enables direct attachment of chips to printed circuit boards through solder joints. The gap between the chip and board is encapsulated with an underfill resin to improve the mechanical, thermal, and structural performance of the package, which in turn enhances the reliability and service life of the electronic device. During the curing process of underfill resin, large residual stresses are generated, and thus significant attention has been placed on understanding the nature and sources of residual stresses in this emerging package type. Residual stresses arise primarily due to the volumetric shrinkage of polymer, as a result of evaporation of solvents and volatile byproducts, cross-linking reaction, and differential thermal shrinkage between different components upon cooling from processing temperature,[1] among which the CTE mismatch is the major source. As shrinkage is constrained by adhesion between the components, residual stress fields are developed across the package, depending on several factors, including the CTEs and elastic modulus of the respective components.

Numerical methods have been widely employed to evaluate the residual stress state in the package and ultimately to optimize the CTEs of underfill resin for improved package reliability.[2,3] The presence of residual stresses has a detrimental effect on the interfacial bond integrity as it allows premature delaminations. Die cracking is another major concern arising from the high stresses concentrated near the die corner. It was proposed that a close match of CTEs between the underfill resin and solder joint is beneficial.[4] Lowering the modulus, CTE, and glass transition temperature, T_g, of underfill resin are found to reduce the residual stress level significantly.[5] A high cooling rate also imparts an adverse effect on the generation of residual stresses.[6] However, as suggested previously,[7] shrinkage in encapsulant may have a beneficial effect of preventing the penetration of water along the interface, enhancing the device reliability against early corrosion failure in the high humidity environment.

Correspondence to: J. K. Kim (mejkkim@ust.hk).

© 2005 Wiley Periodicals, Inc.

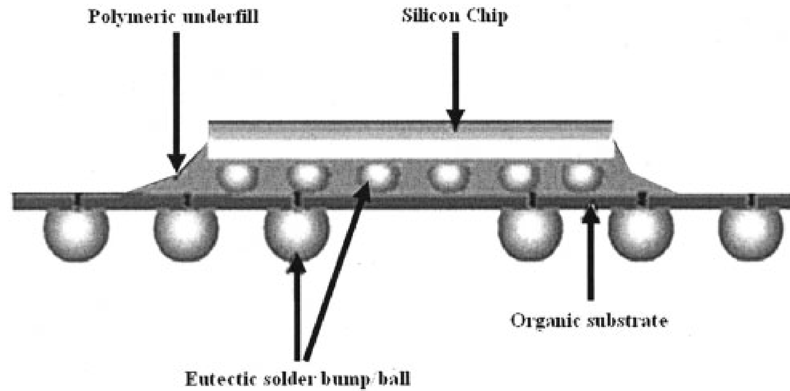

Figure 1 Flip chip on board (FCOB) package configuration.

Significant research has been made toward developing proper techniques to measure residual stresses in electronic package components. These techniques include the blind-hole drilling method,[8] package warpage measurement,[9–11] Moire interferometry,[12–14] and piezoresistive stress sensing IC device.[15–17] The first two techniques are capable of measuring the macroscopic residual stresses in the package, whereas the Moire interferometry and the stress chip method are suitable for measuring the whole-field in-plane displacements over the stresses device. However, wide applications of the latter two techniques have been hindered due to the difficulties involved in replicating the grating on the sample surface at a stress-free elevated temperature and the rigorous requirements in calibrating the piezoresistors at high temperature, respectively.

The present study is aimed to establish the correlation between the curing process and the evolution of process-induced residual stresses in flip chip on board packages by means of several approaches, including the bimaterial bending experiments and rheology measurement. In the bending experiment of resin-substrate bimaterial strips, the radius of curvature of strip is continuously monitored as a function of temperature to predict the generation of residual stresses of chemical and thermal origins.

EXPERIMENTAL

A typical underfill resin (supplied by Dexter Electronic Materials) was employed throughout the study. The resin contained a variety of constituents, including bisphenol F epoxy resin with substituted phthalic anhydride as curing agent and 50% fused silica particles to reduce the CTE of the epoxy. The recommended curing cycle was 7 min at 160°C, and the glass transition temperature of cured resin is reported to be 148°C. The viscosity of underfill resin during the initial stage of curing process was measured on a Physica-UDS200 rheometer equipped with a temperature chamber. The rheometer was operated in the oscillatory parallel-plate geometry with a replaceable aluminium disk. The strain amplitude was 5% at an angular frequency of 100/s. The underfill resin was heated from 40 to 250°C at 10°C/min while monitoring the complex viscosity. In conjunction with the rheology study, a differential scanning calorimeter (Setaram DSC 92) and a thermogravimetric analyzer (Perkin–Elmer TGA 7) were also employed to study the curing kinetics of underfill resin for the identical heating profile.

The bimaterial strip bending experiments (BMSB) and flexural tests of cured resin were carried out *in situ* within a dynamic mechanical analyzer (Perkin–Elmer Pyris DMA7e). The DMA instrument was equipped with a central core rod connecting to a high sensitivity displacement detector (LVDT), a precise linear high force motor, and a low mass, fast-response furnace, as illustrated in Figure 2. Various approaches have been used previously to measure the curvature changes arising from the adhesive curing, for example, optical/laser measurements,[18] telescopic mea-

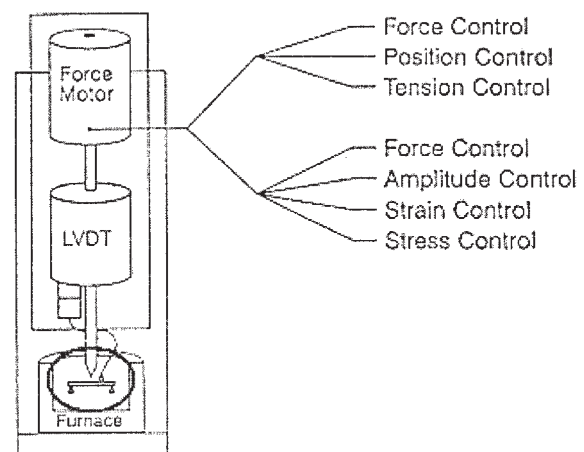

Figure 2 Schematic drawing of the dynamic mechanical analyzer (DMA).

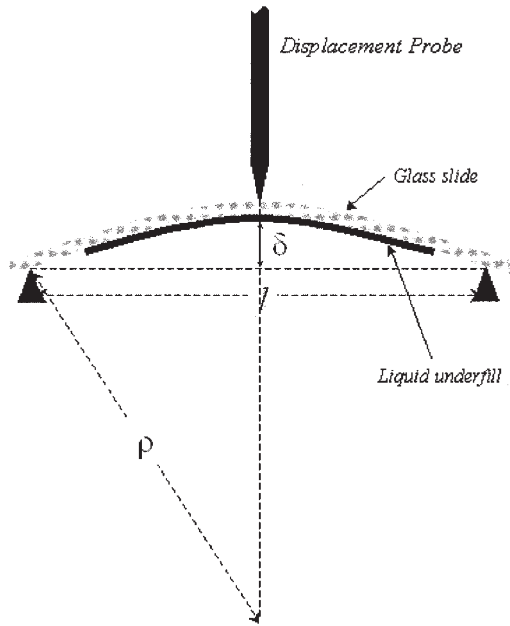

Figure 3 Bimaterial beam bending test configuration.

surement,[19,20] strain gauge measurement,[21] and probe displacement measurement.[22] A three-point bending configuration was used in both experiments with a span length $l = 15$ mm. In the bimaterial strip bending experiment, a thin film of resin was applied onto a 150 μm thick × 18 mm wide × 8 mm long glass slide, as shown in Figure 3. Different from a typical flip chip device configuration as seen previously in Figure 1, the bending of the BMSB specimen was merely due to the differences in CTEs between the glass slide and the epoxy. Hence, hereafter the strain of the epoxy layer in this study is referred as the thermal strain of the epoxy experiencing the temperature change from cure temperature to lower temperature, while the stress in the epoxy layer is induced due to the differences in dimensional changes between the glass slide and the epoxy during thermal excursions. In this sense even though the stress level in the epoxy layer is not directly corresponding to the actual condition in flip chip package, the thermal strain of the epoxy is basically the same in any case, and the residual stress due to the constraints by adhesion between components in the package can then be predicted.

The resin was spin-coated at about 60°C to allow easy spreading and uniform thickness across the whole slide area. Glass was chosen as the substrate material for its stability over the testing temperature with a very low CTE value (5.87 ppm/°C). The resin thickness was about 17 μm as measured using a profilometer. The contact force applied by the displacement probe over the glass surface was 20 mN, and the probe displacement in the midspan of bimaterial strip was continuously monitored against temperature change. The heating and cooling rates used over the whole experiment were both 10°C/min, which are the same as in other thermo-mechanical experiments.

Three-point flexural tests were conducted on cured underfill resin samples at a temperature range between 20 and 240°C to determine the temperature-dependent flexural modulus of the resin. 2 mm thick × 9 mm wide × 18 mm long samples were placed on the bending platform in the DMA chamber to allow temperature equilibrium in the sample before loading. A linearly increasing load was applied from 0.5 to 1.2 N at a rate of 0.1 N/min. The flexural modulus was determined from the linear region of the stress–strain curve at temperatures ranging from 20 to 230°C. The CTE of resin was also measured independently using a thermomechanical analyzer (Mettler Toledo TMA/SPTA 840), allowing direct comparison with that obtained from the bimaterial strip bending experiment.

RESULTS AND DISCUSSION

Correlation between Viscosity and Curing Characteristics of Underfill Resin

Figure 4 shows the change of viscosity with temperature at a temperature range between 50 and 250°C. The viscosity decreased gradually until the tempera-

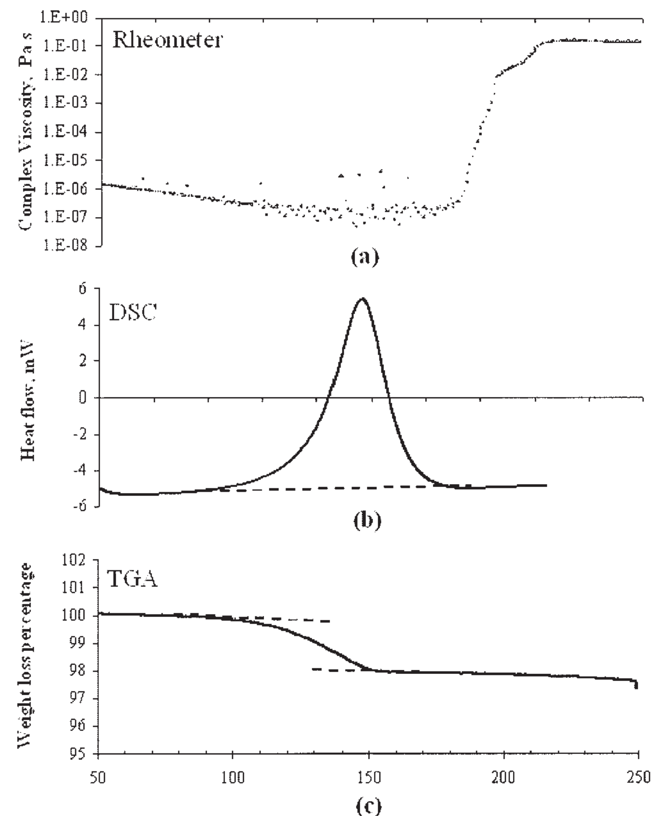

Figure 4 Comparisons of the results on curing the liquid underfill resin by (a) rheometer, (b) DSC, and (c) TGA (heating rate: 10°C/min).

ture reached about 182°C, followed by a rapid surge at higher temperatures. The viscosity of underfill resin depends on a number of factors, such as the formulation of base resin, cure kinetics, as well as the silica filler content and the amounts of volatile solvents. The decrease in viscosity upon initial heating was due in part to enhanced chain segment mobility of the resin molecules.[23–25] For the same reason, there was significant fluctuation of viscosity at temperatures between 130 and 165°C. On the other hand, the continuously increasing temperature accelerated the reaction kinetics of resin until extensive cross-linking was developed, as indicated by the jump in viscosity.[24] The curing process seems to have been almost completed at about 210°C, where the viscosity became a constant plateau value.

Several interesting features were revealed when the viscosity measurements were compared with the DSC and TGA results for the same temperature range. The onset temperature for exothermic reaction (from DSC) at approximately 85°C agreed well with the onset temperature for weight loss (from TGA), which is most likely attributed to the beginning of solvent evaporation in the resin. The reaction rate was the highest at about 150°C as suggested by the DSC result, where the viscosity also showed significant fluctuations. The resin started solidification at about 182°C, as indicated by the viscosity jump in the rheology study, which corresponded to the exit temperature for exothermic reaction (from DSC). This temperature was also equivalent roughly to the end of weight loss (from TGA).

Evolution of Residual Stresses

Figure 5 plots the change of complex viscosity and the corresponding probe displacement arising from shrinkage of resin as measured from the bimaterial strip bending experiments. When the resin was subjected to a linear temperature increase at the initial stage of the curing process, the viscosity decreased due mainly to the evaporation of solvent. This is followed by an almost constant minimum value with some fluctuation between 130 and 160°C, as seen in Figure 5. The viscosity increased rapidly after 2 min of isothermal heating at 160°C as a result of accelerated reaction kinetics[24] and remained steady at over 10^5 Pa · s.

In contrast to the viscosity profile, there was no appreciable increase in the corresponding probe displacement even after isothermal curing at 160°C for 7 min: it started to pick up after the sample was cooled down from the isothermal temperature. This suggests that volume change due to the chemical shrinkage and evaporation of volatiles of the resin were minute. It is understood that, for epoxy resin, the chemical component of shrinkage is normally much smaller than the

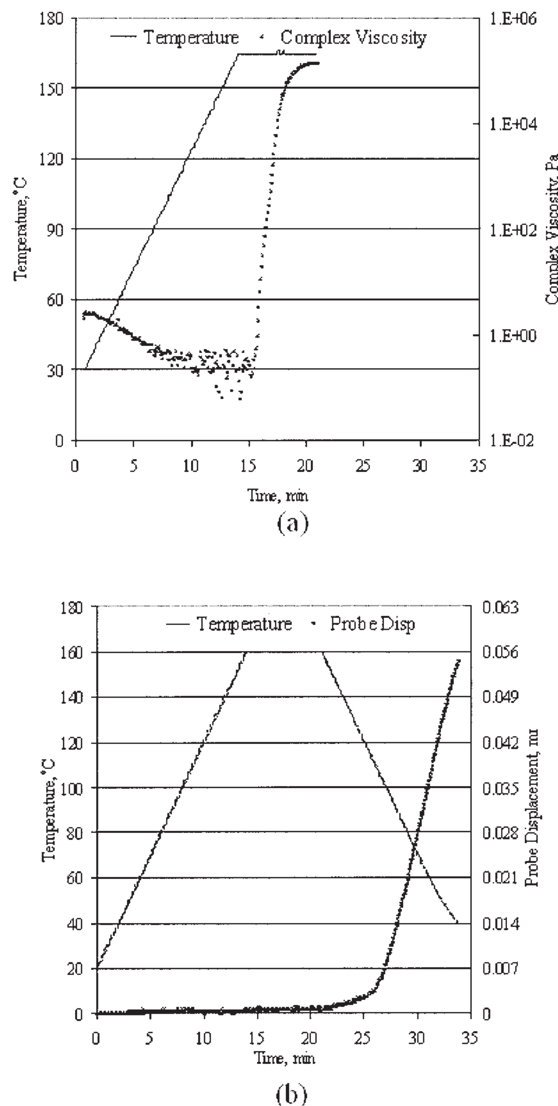

Figure 5 Changes of (a) viscosity and (b) probe displacement with temperature upon isothermal curing and cooling.

thermal origin.[26] Further studies are warranted to properly illustrate the evolution of shrinkage stresses arising from chemical origin, including those due to evaporation of solvent and cross-linking. The displacement exhibited a rapid, linear increase at temperatures below about 115°C.

Based on the simple beam bending theory,[27] the residual stresses, σ, in the resin layer for the bimaterial strip is approximately given:[28]

$$\sigma_a = \frac{1}{\rho}\frac{E_s h_s}{6(1+m)m}\left[\left(1+\frac{6y}{h_a}\right)nm^3 + \frac{6y}{h_a}nm^2 + 1\right] \quad (1)$$

where E and h are the modulus and thickness; and the subscripts s and a refer to the glass substrate and underfill resin, respectively. $m = h_a/h_s$ is the thickness ratio, and n is the moduli ratio E_s/E_s. For a very thin

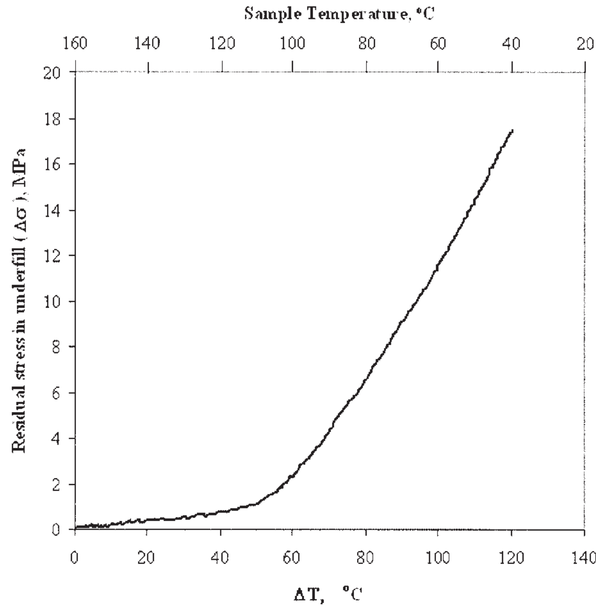

Figure 6 Variation of residual stress in the resin layer as a function of temperature decrement, ΔT, during cooling.

resin layer over the glass slide, i.e., $h_a \ll h_s$, the residual stress in the resin layer can be further simplified:

$$\sigma_a = \frac{1}{\rho} \times \frac{E_s \times h_s^2}{6 \times h_a} \tag{2}$$

The radius of curvature, ρ, of the bimaterial strip can be obtained directly from the bending geometry as a function of midspan displacement, δ, as follow:

$$\rho = \frac{l^2}{8\delta} + \frac{\delta}{2} \approx \frac{l^2}{8\delta} \tag{3}$$

where l is the span length of the bending platform, see Figure 3. Therefore, substitution of eq. (3) into eq. (2) gives:

$$\sigma_a = \frac{4}{3} \times \frac{E_s \times h_s^2}{h_a l^2} \delta \tag{4}$$

Figure 6 plots the variations of residual stress in the resin layer as a function of temperature decrement, ΔT, from the isothermal temperature. Table I summarizes the material properties and specimen parameters used for the residual stress calculation. While the general trend of residual stress with temperature change in Figure 6 looks basically similar to that for the probe displacement [Fig. 5(b)], the stress profile showed approximately a bilinear variation at two distinct temperature regions. At temperatures above about 115°C, the residual stress increase was moderate due mainly to the rubbery state of polymer where the elastic modulus is very low (although the CTE value may be even higher than that below T_g). In contrast, the transition from the rubbery to glassy state when the temperature was well below 115°C induced a rapid increase in residual stress.

TABLE I
Material Parameters for the Internal Stress Calculation for the Underfill Layer

Flexural modulus of glass slide (E_{sub}): 41.23 GPa at room temperature
Thickness of glass slide, h_s: 150 μm
Thickness of resin layer, h_a: 17 μm
$\upsilon_s = 0.2$; $\upsilon_a = 0.35$
CTE of glass, α_s: 5.87 ppm/°C
Relationship between the residual stress, σ_a, and beam deflection, δ
$\sigma = 3.234 \times 10^{11}\ \delta$ (Pa)

The bending of the bimaterial strip upon cooling from the isothermal temperature was mainly due to the mismatches in CTE between the glass substrate, α_s, and resin layer, α_a. The thermal mismatch stress in the resin layer was predicted previously[29] based on the constitutive equations, which are further modified taking into account the contributions by the substrate material as shown in the Appendix:

$$\sigma_a = \frac{E_a}{(1 - \upsilon_a)} [\alpha_a - \alpha_s] \Delta T \tag{5}$$

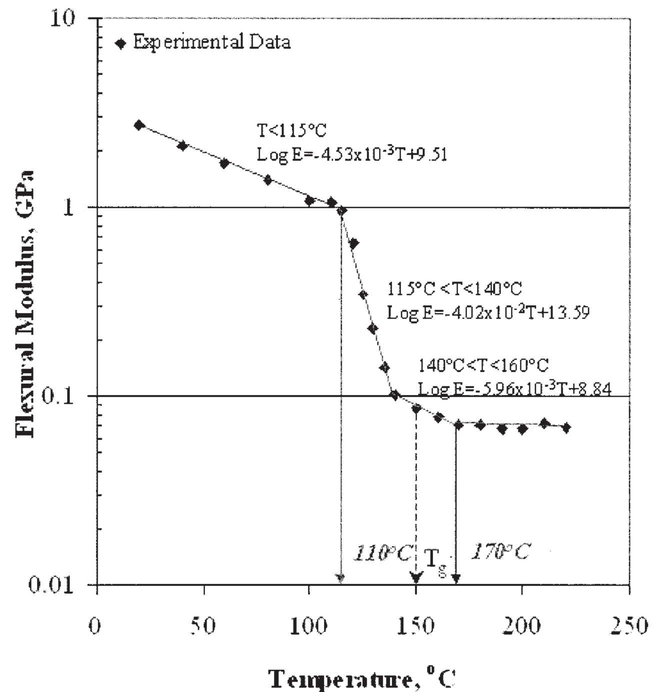

Figure 7 Variation of flexural modulus of cured resin with temperature.

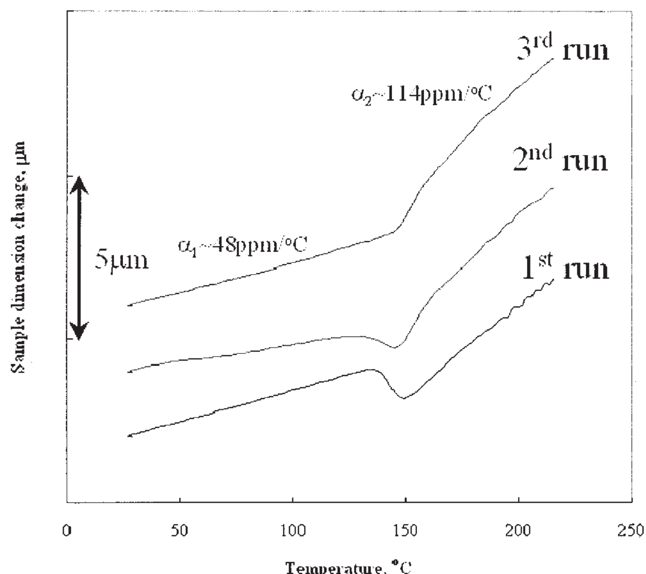

Figure 8 Variations of sample dimensions measured from TMA.

where υ is the Poisson ratio. By rearranging eq. (5), the CTE of resin, α_a, is given:

$$\alpha_a = \alpha_s - \frac{\sigma_a(1 - \upsilon_a)}{E_a \times \Delta T} \quad (6)$$

To estimate the CTE of resin based on eq. (6), the temperature-dependent elastic modulus of resin, E_a, must be known. Thus, the elastic moduli of resin were measured in three-point flexure tests of cured resin *in situ* the DMA chamber and are plotted in Figure 7 on a logarithmic scale. As expected, the flexural modulus decreased characteristically as temperature increased. It decreased rather slowly in a linear manner until the temperature reached about 115°C. There was a transition region between temperatures 115 and 170°C where the modulus changed parabolically. A glass transition temperature, $T_g \approx 147$°C, was determined at approximately the midpoint of this temperature range, which is exactly the same as $T_g \approx 147$°C reported by the material supplier. The flexural modulus became almost a constant plateau value at above 170°C.

Coefficient of Thermal Expansion

The dimensional changes of the underfill resin obtained from the TMA experiment is plotted as a function of temperature in Figure 8; and the CTE profile calculated based on eq. (6) is given in Figure 9. There are a few points of interest worth mentioning. The "hill" and "valley" phenomenon was observed in the TMA plot, which was thought to be associated with the relaxation of residual stress–strain following the collapse of the frozen-in excess free volume of the polymer.[14] The multiple displacement profiles shown in Figure 8 represent those obtained in three consecutive temperature excursions in the TMA experiments, with diminishing "hill" and "valley" fluctuations in the later tests. It is remarkable to note that the CTE values determined from all sources for the low temperature range were essentially identical each other: α_1 = 48 ppm/°C from the material supplier, 51 ppm/°C from the stress measurement, and 48 ppm/°C from the TMA. This confirms in part the validity of the bimaterial strip bending test. While the CTE is constant at temperatures below 70°C, it reached a minimum value of 39 ppm/°C at about 115°C (Fig. 9). This anomaly reflects the sharp drop in flexural modulus at a temperature corresponding to the T_g of the underfill resin (see Fig. 7). There was an irregular variation of CTE profile, with its value varying between 100 to 280 ppm/°C, at temperatures above 140°C. This appears to be associated with the equation used to calculate the residual stress, which was based on the assumption of linear elastic material properties, while the underfill resin actually is highly viscous in nature when the temperature was above T_g. In this regard, the residual stress and the CTE values presented in this work may become accurate in the high temperature range.

CONCLUSION

The rheology and curing characteristics of an underfill resin were evaluated based on the rheometer, DSC, and TGA analyses, and correlations were established between the results obtained. The bimaterial bending

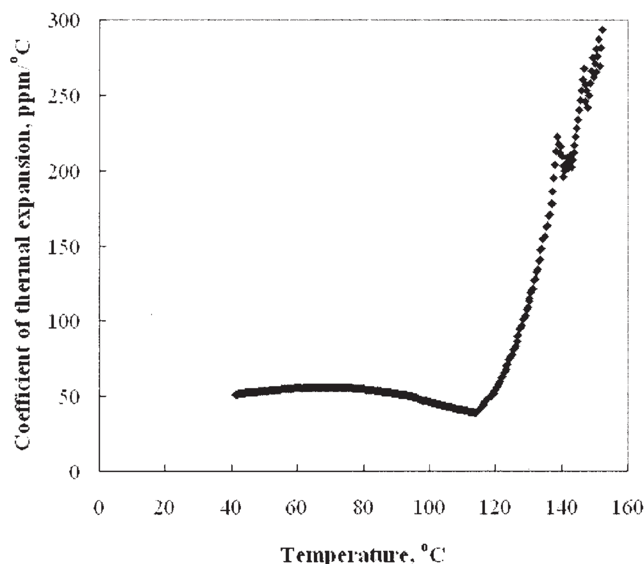

Figure 9 Coefficient of thermal expansion of resin with temperature from BMSB test.

experiments were successfully carried out to monitor *in situ* the evolution of residual stresses in the resin, which is subjected to typical curing and cooling temperature excursions. The CTEs were determined based on the simple thermomechanical analysis of residual stress profiles, which are compared with those obtained from other sources. The following remarks can be highlighted.

1. The results obtained from the DSC, TGA, and rheology analyses were well correlated: the onset of exothermic reaction corresponded to the beginning of weight loss, while the sharp change in viscosity corresponded to the completeness of exothermic reaction.
2. The residual stress profile showed approximately a bilinear variation at two distinct temperature regions: at high temperatures above 115°C the residual stress increased moderately due to the rubbery state of polymer, and the glassy state of polymer at temperatures below 115°C induced a rapid increase in residual stress.
3. The CTE value for temperatures below about 70°C determined from the bimaterial strip bending experiment, α_1 = 51 ppm/°C, is essentially identical to those reported from the material supplier, α_1 = 48 ppm/°C, and the TMA result, α_1 = 48 ppm/°C. This partly confirms the validity of the bimaterial strip bending test employed in this study.

The authors thank the Research Grant Council for continuous support of this project. Assistance with experiments rendered by the EPack Lab, Materials Characterisation and Preparation Facilities and Advanced Engineering Materials Facilities, HKUST is also gratefully appreciated. Dexter Electronic Materials, Hong Kong, supplied the underfill resin.

APPENDIX: ANALYSIS OF RESIDUAL STRESSES IN A BIMATERIAL STRIP

The bending of a bimaterial strip upon cooling from the isothermal cure temperature in Figure A1 occurs due to the mismatches in CTEs between the glass substrate, α_s, and resin layer, α_a.

The generalized thermoelastic stress–strain relations for three-dimensional problems are:[27]

$$\Delta\varepsilon_x - \alpha\Delta T = \frac{1}{E}\left[\Delta\sigma_x - \upsilon(\Delta\sigma_y + \Delta\sigma_z)\right] \quad \text{(A1a)}$$

$$\Delta\varepsilon_y - \alpha\Delta T = \frac{1}{E}\left[\Delta\sigma_y - \upsilon(\Delta\sigma_x + \Delta\sigma_z)\right] \quad \text{(A1b)}$$

$$\Delta\varepsilon_z - \alpha\Delta T = \frac{1}{E}\left[\Delta\sigma_z - \upsilon(\Delta\sigma_x + \Delta\sigma_y)\right] \quad \text{(A1c)}$$

$$\Delta\gamma_{xy} = \frac{\Delta\tau_{xy}}{G}\ \Delta\gamma_{yz} = \frac{\Delta\tau_{yz}}{G}\ \Delta\gamma_{xz} = \frac{\Delta\tau_{xz}}{G} \quad \text{(A1d)}$$

Plane stress will occur in a thin plate when the temperature does not vary through the thickness, therefore we may assume that $\Delta\sigma_z = \Delta\tau_{xz} = \Delta\tau_{yz} = 0$. We may also regard each element as free to expand in the z direction. As suggested in the method of strain suppression on a thin plate,[27] thermal expansions are considered only in the x and y directions with the following relationships:

$$\Delta\sigma_x = \Delta\sigma_y \text{ and } \Delta\tau_{xy} = 0 \quad \text{(A2)}$$

Hence, from eq. (A1),

$$\Delta\varepsilon_x = \Delta\varepsilon_y = \frac{\Delta\sigma_x}{E}\left[1 - \upsilon\right] + \alpha\Delta T \quad \text{(A3)}$$

The stress and strain in eq. (A3) should be interpreted as quantities averaged through the thickness, of which the case is referred to as generalized plane stress.[27] For small curvature, the compatibility condition requires that ε_x in the adhesive layer and the substrate are the same: $[\Delta\varepsilon_x]_a = [\Delta\varepsilon_x]_s$.

$$\Delta\varepsilon_x = \frac{[\Delta\sigma_x]_s}{E_s}\left[1 - \upsilon_s\right] + \alpha_s\Delta T = \frac{[\Delta\sigma_x]_a}{E_a}\left[1 - \upsilon_a\right] + \alpha_a\Delta T \quad \text{(A4)}$$

where the subscripts s and a refer to the substrate and adhesive, respectively. For force balance in the absence of the external stresses,[29]

$$h_a[\Delta\sigma_x]_a + h_s[\Delta\sigma_x]_s = 0 \quad \text{(A5a)}$$

Figure A1 Bimaterial strip.

Thus,

$$[\Delta\sigma_x]_s = -\frac{h_a}{h_s}[\Delta\sigma_x]_a = -m[\Delta\sigma_x]_a \quad \text{(A5b)}$$

where $m = h_a/h_s$. Therefore, combining eqs. (A4) and (A5b) gives,

$$[\Delta\sigma_x]_a\{(1-\upsilon_a) + mn(1-\upsilon_s)\} = E_a(\alpha_s - \alpha_a)\Delta T \quad \text{(A6)}$$

where $n = E_a/E_s$. By approximation, $mn \approx 0$, then

$$\alpha_a = \alpha_s - \frac{[\Delta\sigma_x]_a}{E_a\Delta T}(1-\upsilon_a) \quad \text{(A7)}$$

It follows that once the residual stress $[\Delta\sigma_x]_a$ [which is the same as σ_a in eq. (4)] is obtained from the curvature measurement, and the temperature-dependent elastic modulus of adhesive, E_a, is measured, the *in situ* change of CTE of the adhesive layer α_a can be determined.

References

1. Soane, D. S. Chem Eng Prog 1990, 28, 28.
2. Pang, J. K. L.; Tan, T. I.; Chong, Y. R.; Lim, G. Y.; Wong, C. L. J Electron Manufact 1998, 8, 181.
3. Gektin, V.; Bar-Cohen, A.; Witzman, S. IEEE Trans Compon Packag Manufact Technol A 1998, 21, 577.
4. Lu, J.; Wu, J.; Liew, Y. P.; Lim, T. B.; Zong, X. In Proceedings of the 3rd International Symposium on Electronics Packaging Technology 1998, 311–316.
5. Bair, H. E.; Boyle, D. J.; Ryan, J. T.; Taylor, C. R.; Crouthamel, D. L. Polym Eng Sci 1990, 30, 609.
6. Chung, H.; Lee, J.; Jang, W.; Shul, Y.; Han, H. J Polym Sci B 2000, 38, 2879.
7. Bolger, J. C. In Proceedings of the 47th Electronic Components and Technology Conference 1997, 842–849.
8. Wu, Z.; Lu, J.; Guo, Y. J Electron Packag 2000, 122, 262.
9. Kong, J. W. Y.; Kim, J. K.; Yuen, M. M. F. IEEE Trans Compon Packag Manufact Technol C 2003, 26, 245.
10. Suhir, E. J Electron Packag 1992, 114, 467.
11. Suhir, E.; Manzione, L. T. J Electron Packag 1992, 114, 329.
12. Liu, S.; Zhu, J.; Zou, D.; Benson, J. IEEE Trans Compon Packag Manufact Technol A 1997, 20, 505.
13. Zhang, W.; Wu, D.; Su, B.; Hareb, S. A.; Lee, Y. C.; Masterson, B. P. IEEE Trans Compon Packag Manufact Technol A 1998, 21, 323.
14. Li, S.; Shen, J.; Chen, X.; Chen, R.; Luo, X. J Macro Sci Phys 1997, B36, 357.
15. Zou, Y.; Suhling, J. C.; Johnson, R. W.; Jaeger, R. C.; Mian, A. K. M. IEEE Trans Electron Packag Manufact 1999, 22, 38.
16. Palaniappan, P.; Baldwin, D. F.; Selman, P. J.; Wu, J.; Wong, C. P. IEEE Trans Electron Packag Manufact 1999, 22, 53.
17. Palaniappan, P.; Baldwin, D. F. Microelectron Reliab 2000, 40, 1181.
18. Du, Y.; Zhao, J.; Ho, P. J Electron Packag 2001, 123, 196.
19. van den Bogert, W. F.; Molter, M. J.; Gee, S. A.; Belton, D. J.; Akylas, V. R. In Polymeric Materials for Electronics Packaging and Interconnection; Lupiuski, J. H.; Moore, R. S., Eds.; American Chemistry Society: Washington, DC, 1989; Ch. 28.
20. Biernath, R. W.; Soane, D. S. In Polymeric Materials for Electronics Packaging and Interconnection; Lupiuski, J. H.; Moore, R. S., Eds.; American Chemistry Society: Washington, DC, 1989; Ch. 29.
21. Djokic, D.; Johnston, A.; Rogers, A.; Lee-Sullivan, P.; Mrad, N. Composites A 2002, 33, 277.
22. Wang, H.; Yang, Y.; Yu, H.; Sun, W.; Zhang, Y.; Zhou, H. Polym Eng Sci 1995, 35, 1895.
23. Chung, H.; Lee, J.; Shul, Y.; Han, H. J Polym Sci B 2000, 38, 2879.
24. Bidstrup-Allen, S. A.; Wang, S.; Nguyen, L. T.; Arbelaez, F., In Proceedings of the 1st IEEE International Symposium on Polymer Electronic Packaging 1997, 149.
25. Fuller, B.; Gotro, J. T.; Martin, G. C. In Polymer Characterization Physical Property, Spectroscopic, and Chromatographic Methods; Crarer, C. D.; Provder, T., Eds.; American Chemistry Society: Washington DC, 1990; Ch. 12.
26. Kelly, G.; Lyden, C.; Lawton, C.; Barrett, J.; Saboui, A.; Exposito, J.; Lamourelle, F. In Proceedings of the 44th Electronic Components and Technology Conference 1994, 102–106.
27. Timoshenko, S. P.; Goodier, J. N. Theory of Elasticity; McGraw Hill, 1970.
28. Nakamura, Y.; Tabata, H.; Suzuki, H.; Iko, K.; Okube, M.; Matsumoto, T. J Appl Polym Sci 1986, 32, 4865.
29. Hsueh, C. H.; Evans, A. G. J Am Ceram Soc 1985, 68, 241.